

Fractal-Like Behavior of a Mass-Transport Process

Masahiro Kinoshita, Makoto Harada, Yasuo Sato, Kyoichi Tsubata, and Yasutaka Nakamura

Advanced Energy Utilization Division, Inst. of Advanced Energy, Kyoto University, Uji-shi, Kyoto-fu 611, Japan

After an aqueous solution containing Sr^{2+} was flowed through a bed packed with particles of activated charcoal for a very long time, the flow was abruptly switched to deionized water. The variation in ionic concentration at the outlet with time was characterized by the power law, $C_{\text{out}} \sim t^{-\alpha}$, for sufficiently large t . This fractal-like behavior we reported previously has further been studied theoretically and experimentally. A major concern is to examine dependency of α on experimental conditions. Adsorption sites predominate over dead-end pores or spaces as "trappers" in our case where Sr^{2+} or Ba^{2+} is adsorbed on activated charcoal. The experimental results can well be explained by our theoretical model. It has been found, however, that the response curve for Sr^{2+} deviates from the power law after a very long time. This deviation can be explained by introducing the assumption that there exists a maximum value of the activation energy for the desorption process. The curve for Ba^{2+} , on the other hand, exhibits no such deviation until C_{out} decreases to the detection limit of the analytical device used.

Introduction

In an earlier article (Kinoshita et al., 1992), we reported a striking example of an anomalous behavior observed in a preliminary response experiment for a packed bed, and proposed a simple, new model for elucidating the behavior. In the experiment, a column packed with activated charcoal particles served as the packed bed. First, an aqueous solution containing Sr^{2+} was flowed through the bed for about two weeks, and then the flow was abruptly switched to deionized water. The response, the variation of C_{out} (ppm) with t (time, min) was characterized by the power law

$$C_{\text{out}} \sim t^{-\alpha}, \quad (t \rightarrow \text{sufficiently large}) \quad (1)$$

which did not follow from a conventional theory. C_{out} is the concentration of cations at the outlet of the packed bed, ppm. We note that such a power law is very hard to notice from usual breakthrough curves obtained from a step response. Instead, an inverse step response mentioned above or an impulse response must be employed, and a long-time behavior is to be studied by plotting the relation between $\log(C_{\text{out}})$ and $\log(t)$. The behavior expressed by Eq. 1 was called "fractal-like" after the electron-hole transport through amorphous materials (Scher and Montroll, 1975; Noolandi, 1977; Pfister and Scher, 1978), the diffusion-controlled chemical re-

actions within glassy matrices (Plonka, 1986), and those inside porous polymeric membranes and porous glasses (Kopelman, 1986, 1989). These are all categorized as dynamical processes within disordered or nonhomogeneous media (Freeman, 1987).

Our model reported in the previous article considers a general situation where a fluid flows through disordered or nonhomogeneous media and solute molecules or ions in the fluid move with the flow being trapped on adsorption sites (class 1) and dead-end pores or spaces (class 2) and released from these trappers. We note that the two classes of trappers are treated separately in the model. Although the interplay of the two classes of trappers could be significant in the actual situations, two extreme cases can be summarized as follows. When the adsorption sites dominate, the exponent α in Eq. 1 is approximately given by

$$\alpha = T/T_c, \quad (2)$$

where T_c is a constant (K) depending on the adsorbent and solute species, and α varies almost in proportion to the absolute temperature T (K). A change in solute species results in a change in T_c , and a different value of α is observed. On the other hand, when the dead-end pores or spaces dominate, α is only related to geometric aspects of the pores or spaces and independent of T . If both of the two classes of

Correspondence concerning this article should be addressed to M. Kinoshita.

trappers make significant contribution to the transport process, α should exhibit some complicated, intermediate dependency on T .

Another significant prediction of our model is that α in Eq. 1 is not affected by the flow rate, bed length, and initial concentration of the solute molecules or ions. However, this prediction has not been verified yet. In this article we report a new set of data of response experiments performed under a variety of conditions and a further examination of our model. We are particularly concerned with the following subjects: (1) dependency of α on the experimental conditions such as the water flow rate, bed length, initial concentration of cations, cation species (Sr^{2+} and Ba^{2+}) and operating temperature; (2) possibility of the interplay of the two classes of trappers; and (3) study of whether the power law holds until $t \rightarrow \infty$ or not.

Theoretical Model

We revisit our model (Kinoshita et al., 1992) for the adsorption sites. The desorption of a solute molecule from a site is an activation process, and the inverse of the desorption rate constant w (min) is given by

$$w = w_0 \exp[E/(RT)] \quad (3)$$

Assuming that E obeys a completely random distribution

$$q(E) = q_0 \exp[-E/(RT_c)], \quad q_0 = 1/(RT_c) \quad (4)$$

and using the relation $q(E)dE = h(w)dw$, we obtain

$$h(w) \sim w^{-1-T/T_c} \quad (5)$$

$X \sim Y$ means that X is proportional to Y (except in the regions of extremely small Y and extremely large Y). However, there should be a minimum value E_{\min} (J/mol) and a maximum value E_{\max} (J/mol) for the activation energy. Hence, Eq. 5 is valid only for $w_{\min} < w < w_{\max}$. We then express the distribution of the residence time by

$$\phi_1(t, w) = (1/w) \exp(-t/w) \quad (6)$$

Equation 6 is based on the idea that the residence time of a solute molecule adsorbed on a site having a certain activation energy cannot uniquely be determined because the desorption is a stochastic process: some solute molecules are released shortly, while others spend a rather long time on the site. Then, the overall residence-time distribution function $\Phi_1(t)$ (1/min) is given by

$$\Phi_1(t) = \int_{w_{\min}}^{w_{\max}} h(w) \phi_1(t, w) dw \sim t^{-1-T/T_c} \int_{t/w_{\max}}^{t/w_{\min}} z^{T/T_c} \exp(-z) dz. \quad (7)$$

Regarding w_{\min} and w_{\max} as nearly zero and infinitely large, respectively, we obtain

$$\int_{t/w_{\max}}^{t/w_{\min}} z^{T/T_c} \exp(-z) dz = \Gamma(T/T_c + 1) \quad (8)$$

where Γ denotes the gamma function and $\Gamma(T/T_c + 1)$ is independent of t . From Eqs. 7 and 8, we obtain

$$\Phi_1(t) \sim \Gamma(T/T_c + 1) t^{-1-T/T_c} \quad (9)$$

As we showed in our previous article, $C_{\text{out}}(t)$ measured in the response experiments is closely related to $\Phi_1(t)$. Assuming that the adsorption sites dominate as trappers results in

$$C_{\text{out}} \sim t^{-T/T_c}, \quad (t \rightarrow \text{sufficiently large}). \quad (10)$$

Next, it is worthwhile to comment on the rate equation (Kinoshita et al., 1992) expressed by

$$\partial \Delta P_1(t, x) / \partial t = \omega \Delta P(t, x) - \int_0^t \omega \Delta P(t-t', x) \Phi_1(t') dt', \quad (11)$$

$$\Delta P_1(t, x) = P_1(t, x) - P_1(0, x), \quad \Delta P(t, x) = P(t, x) - P(0, x). \quad (12)$$

The first and second terms on the righthand side of Eq. 11 denote adsorption and desorption rates, respectively. The use of the first term is valid only in the situations where the concentration of solute molecules or ions is sufficiently low and many of the adsorption sites are vacant, because the adsorption rate is assumed to be proportional to $\Delta P(t, x)$. However, this does not pose any problem as long as we are concerned with the response curves after a sufficiently long time (the situations where the ionic concentration is everywhere sufficiently low). We then discuss the second term on the righthand side of Eq. 11 more closely. The Laplace transform of the second term (the desorption rate) $\tilde{Y}_{\text{out}}(s, x)$ is

$$\tilde{Y}_{\text{out}}(s, x) = \tilde{Y}_{\text{in}}(s, x) \tilde{\Phi}_1(s), \quad \tilde{Y}_{\text{in}}(s, x) = \omega \tilde{\Delta P}(s, x), \quad (13)$$

where $\tilde{Y}_{\text{in}}(s, x)$ is the Laplace transform of the first term (the adsorption rate). The physical meaning of Eq. 13 is now clear. $\tilde{\Phi}_1(s)$ is a transfer function for the system consisting of adsorption sites and relates the desorption rate with adsorption rate at any position x .

Experimental Method

A column (column diameter = 0.8 cm) packed with activated charcoal particles (particle diameter is about 450 μm) serves as a packed bed. Most of the experimental equipment is made of teflon and maintained at a prescribed temperature by a water bath. First, we let an aqueous solution flow through the bed for about two weeks. Then, we abruptly switch the flow to deionized water. Microtube pumps are used before and after the switch. The response, the variation of C_{out} (ppm) with t (min), is measured by the inductively coupled plasma-emission spectroscopy (ICPS). Experiments are performed under various conditions summarized in Table 1. Due to insufficient resistance to the microtubes the flow rate

Table 1. Experimental Conditions

Run No.	Species	C_{in} ppm	F cm ³ /min	L cm	T K
1	Sr ²⁺	50	0.06	5	278
2	Sr ²⁺	50	0.20	5	278
3	Sr ²⁺	50	0.67	5	278
4	Sr ²⁺	50	0.21	10	298
5	Sr ²⁺	500	0.23	10	298
6	Sr ²⁺	50	0.18	20	298
7	Sr ²⁺	10	0.26	5	278
8	Sr ²⁺	50	0.20	5	298
9	Ba ²⁺	50	0.21	5	278
10	Ba ²⁺	50	0.21	5	303

decreased very gradually with time. This caused some scattering of experimental data and some uncertainty of the exponent α determined (the value determined was slightly smaller than the correct value). We therefore changed the microtubes to much more resistant ones. It has been verified that with this treatment the flow rate remains perfectly constant.

In addition to the response experiments summarized above, we measure adsorption equilibrium of Sr²⁺ and Ba²⁺ between aqueous solution and activated charcoal. A prescribed volume of aqueous solution (the ionic concentration C_1 is known) is brought in contact with fresh charcoal particles (with a prescribed total weight). The equilibrium is reached in 50 h. From C_1 and the ionic concentration after the equilibrium is reached, the total amount of the ionic species (Sr²⁺ or Ba²⁺) adsorbed on charcoal is determined.

Results and Discussion

We are concerned with the response curves after sufficiently long time. It has been found that all the responses can be characterized by the power law expressed by Eq. 1. After a very long time, however, C_{out} measured in Runs 1 through 8 (runs for Sr²⁺) appears to decrease more rapidly than the line of the power law. This departure from the power law will be discussed in a later section. Hereafter, we concentrate on the dependency of α on the experimental conditions.

Figure 1 illustrates the effect of the flow rate F (cm³/min). As shown in the figure, when C_{out} is plotted against t/τ (the value of τ in Run 2, for example, is 0.6 min), the three curves are almost indistinguishable. The most significant conclusion is that α is independent of the flow rate in the flow rate range tested. Two curves are compared in Figure 2. Only the initial concentration of Sr²⁺ is different for the two runs. For $t/\tau \geq 10$, the two curves are almost indistinguishable and share the same exponent. A similar comparison is made in Figure 3. For $t/\tau \geq 15$, the curve for the lower initial concentration is somewhat shifted below, but again the two curves share almost the same exponent. Figure 4 shows that the exponent is not affected by the bed length either. Thus, α does not depend on such parameters as the water flow rate, bed length, and initial concentration of cations.

The effect of the operating temperature is now discussed. Figure 5 shows two response curves obtained under two different temperatures, 5°C and 25°C. There is a marked difference between the two curves in α , and the lower temperature leads to a lower value of α . For the ten runs given in Table 1, α has been determined by the least-squares tech-

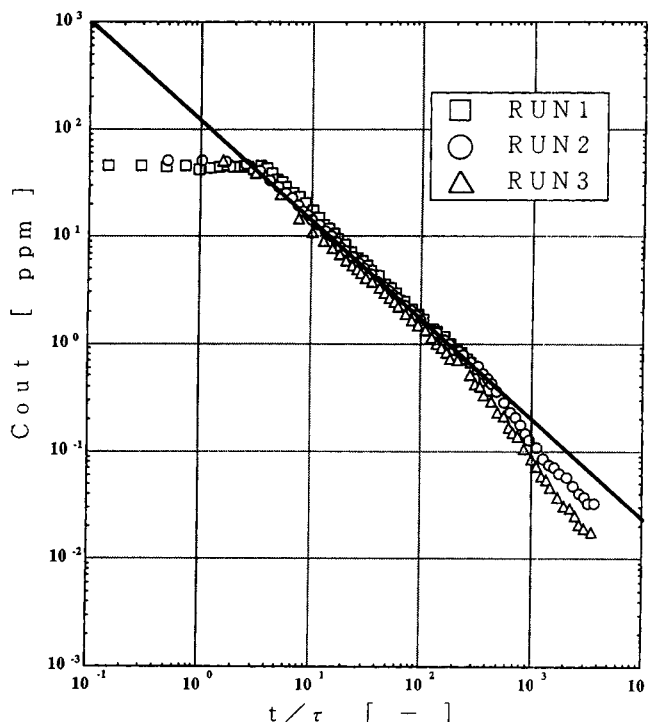


Figure 1. Response curves from Runs 1-3.

τ is the apparent residence time (min) ($\tau = \epsilon LS/Q$). The straight line is drawn for Run 2 and its slope is -0.929 .

nique using the data in the time region where the power law appears to hold. The result obtained is the following:

For Sr²⁺ and 5°C: $\alpha = 0.979$ (average of those from Runs 1-3 and 7).

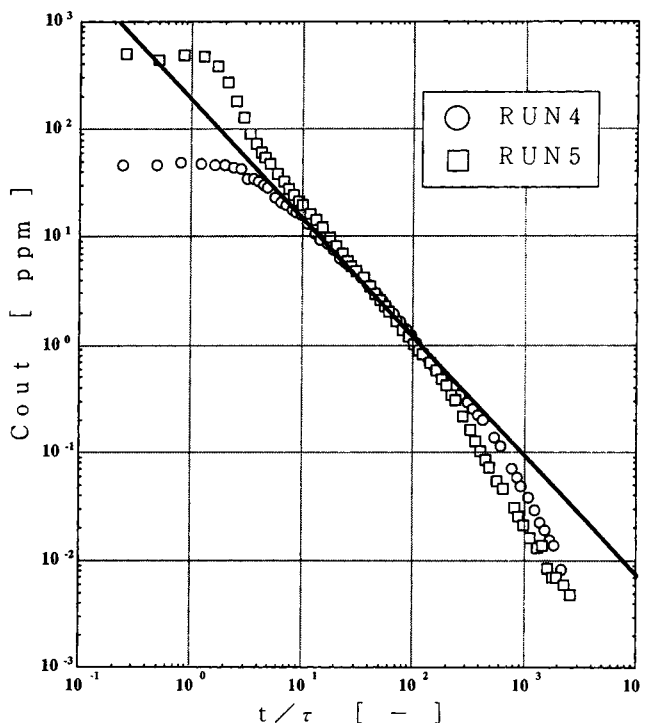


Figure 2. Response curves from Runs 4 and 5.

The straight line is drawn for Run 4 and its slope is -1.10 .

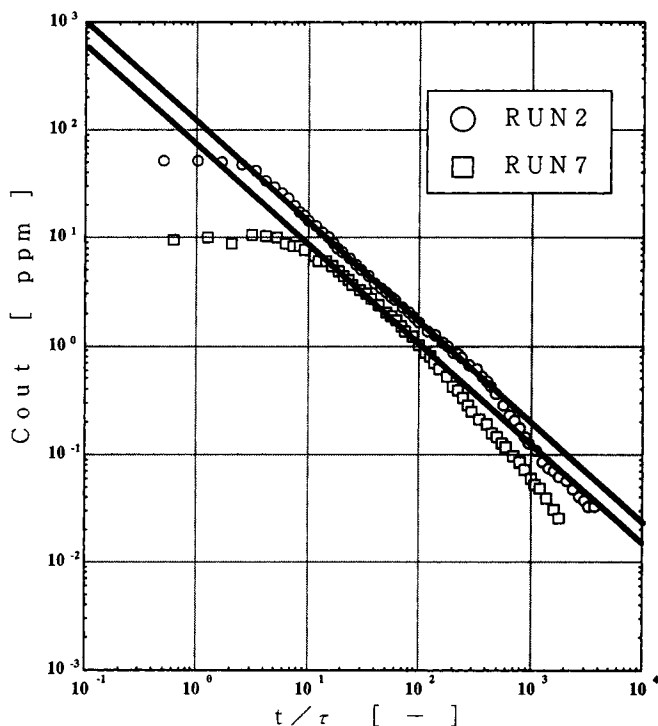


Figure 3. Response curves from Runs 2 and 7.

The slope of the two straight lines drawn is -0.929 .

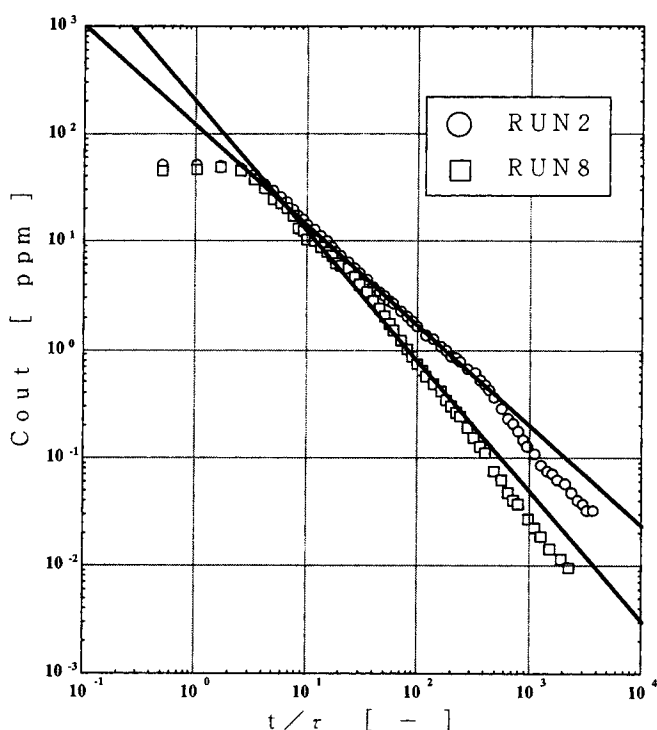


Figure 5. Response curves from Runs 2 and 8.

The slopes of the two straight lines drawn for Runs 2 and 8 are -0.929 and -1.21 , respectively.

For Sr^{2+} and 25°C : $\alpha = 1.19$ (average of those from Runs 4–6 and 8).

For Ba^{2+} and 5°C : $\alpha = 1.26$ (Run 9).

For Ba^{2+} and 30°C : $\alpha = 1.38$ (Run 10).

Figure 6 shows a comparison between two response curves

obtained at 5°C for two different species Sr^{2+} and Ba^{2+} . The exponents in the two runs are clearly different. Thus, α exhibits a clear dependence only on the operating temperature and cation species. We note that for Ba^{2+} the power law is

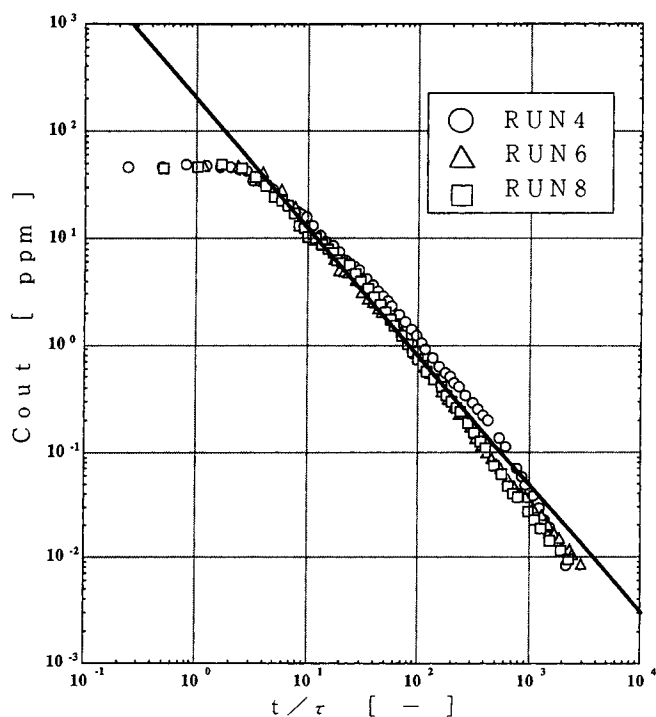


Figure 4. Response curves from Runs 4, 6 and 8.

The straight line is drawn for Run 8 and its slope is -1.21 .

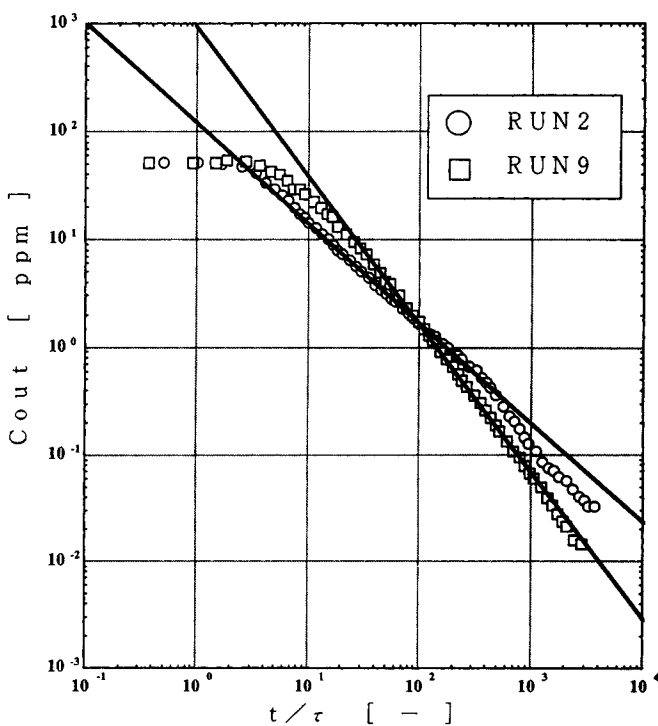


Figure 6. Response curves from Runs 2 and 9.

The slopes of the two straight lines drawn for Runs 2 and 9 are -0.929 and -1.26 , respectively.

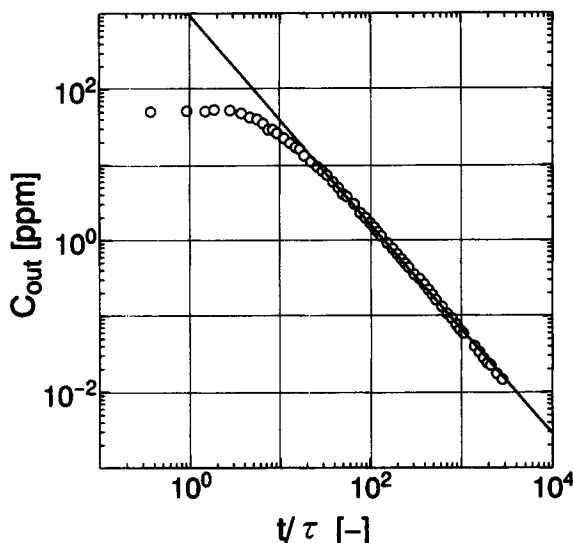


Figure 7. Response curve from Run 10.

The slope of the straight line drawn is -1.38 .

followed until the concentration decreases to the detection limit of ICPS (~ 0.01 ppm), and no departure is observed (see Figure 7, also).

If the effect of the dead-end pores or spaces dominates, α remains unchanged against changes in the operating temperature. On the other hand, if the effect of the adsorption sites is much more important, α is approximately given by Eq. 2. If both of the two classes of trappers contribute significantly to the fractal-like behavior, α should be dependent on T more weakly than Eq. 2 suggests. We employ Eq. 2 and determine T_c for Sr^{2+} and Ba^{2+} with the result that

For Sr^{2+} : $T_c = 280$ K for 5°C and $T_c = 250$ K for 25°C .

For Ba^{2+} : $T_c = 220$ K for 5°C and $T_c = 220$ K for 30°C .

If the experimental results obey Eq. 2 completely, T_c is independent of T . For Ba^{2+} , this is perfectly satisfied, while for Sr^{2+} the results show that the dependency of α on T is stronger than that suggested by Eq. 2. Hence, we can conclude that the adsorption sites are predominant over dead-end pores or spaces in our case (and probably in many other cases also). Considering the simplicity of our model, the agreement between theoretical prediction and experimental observation in terms of the dependency of α on the experimental conditions is very good.

The experimental results of the adsorption equilibrium of Sr^{2+} and Ba^{2+} between the aqueous solution and activated charcoal are now discussed. The data obtained for the equilibrium are plotted in Figure 8. The equilibrium relation can be described by the Freundlich equation

$$X_i = K_i C_i^m. \quad (14)$$

The exponent m determined by the least-squares technique are 0.342 (Sr^{2+} , 5°C), 0.292 (Sr^{2+} , 25°C), 0.360 (Ba^{2+} , 5°C), and 0.295 (Ba^{2+} , 30°C).

Examination of Another Theory

One might think that the power law observed in the response experiments stems from the equilibrium relationship

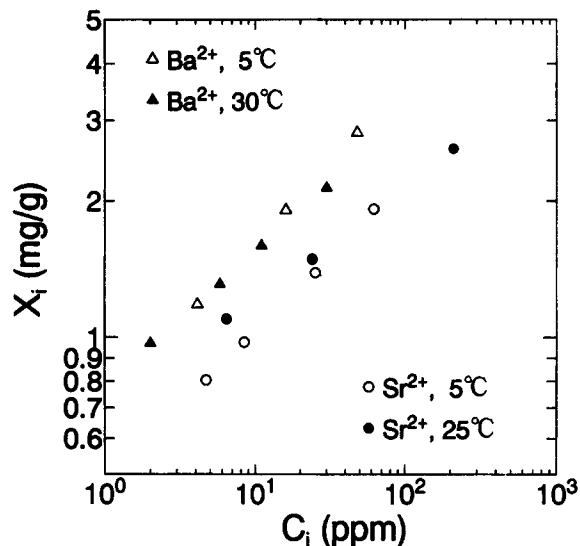


Figure 8. X_i vs. C_i after adsorption equilibrium is reached.

expressed by Eq. 14, which also has a power form. We now examine this thought. As shown in the Appendix, if we assume that adsorption equilibrium always holds between aqueous solution and activated charcoal, and the equilibrium relationship is expressed by the Freundlich equation, we obtain

$$C_{\text{out}} \sim t^{-\alpha}, \quad (t \rightarrow \text{sufficiently large}), \quad \alpha = 1/(1-m). \quad (15)$$

The values of α calculated from Eq. 15 are the following

Sr^{2+} , 5°C : $m = 0.342$, $\alpha = 1.52$ (0.979).

Sr^{2+} , 25°C : $m = 0.292$, $\alpha = 1.41$ (1.19).

Ba^{2+} , 5°C : $m = 0.360$, $\alpha = 1.56$ (1.26).

Ba^{2+} , 30°C : $m = 0.295$, $\alpha = 1.42$ (1.38).

The values in parentheses are those of α determined in the response experiments. The agreement is not good except in the last system. The most significant drawback of Eq. 15 is that α is a decreasing function of T (m is a decreasing function of T), whereas the opposite is true in the results of response experiments. The values of α for Sr^{2+} and Ba^{2+} calculated from Eq. 15 are almost the same, but in the response experiments α for Sr^{2+} are significantly smaller. Moreover, it appears to be unreasonable to assume that adsorption equilibrium always holds, because in the equilibrium experiments over 10 h is needed for the equilibrium to be reached. Equation 15 fails to elucidate the experimental observation. The conclusion is that the power law observed in the response experiments does not stem from the equilibrium relationship expressed by Eq. 14.

Departure from Power Law

A possible explanation of the departure from the power law (Eq. 1) is the following. The minimum volume of dead-end pores or spaces which the solute molecules can enter is not zero, and the maximum volume is finite. Similarly, the solute molecules are not adsorbed on sites with zero activation energy, and sites with an infinitely large activation energy can

Table 2. Relation between t and $\Xi(t)$ for $T/T_c = 1$

t (min)	$\Xi(t)$
0	1.000
0.1 w_{\max}	0.995
0.2 w_{\max}	0.982
0.5 w_{\max}	0.910
1.0 w_{\max}	0.736
2.0 w_{\max}	0.406

hardly exist for the system of cations (Sr^{2+} and Ba^{2+}) and activated charcoal where electrostatic attractions play important roles for the adsorption. (The adsorption is not "chemical" but "physical.") Thus, w_{\min} is not zero and w_{\max} should be finite. We note, however, that w_{\min} and w_{\max} should be very small and very large, respectively. For sufficiently large t

$$\int_{t/w_{\max}}^{t/w_{\min}} z^{T/T_c} \exp(-z) dz = \int_{t/w_{\max}}^{\infty} z^{T/T_c} \exp(-z) dz = \Xi(t) \quad (16)$$

$$\Phi_1(t) \sim \Xi(t)t^{-1-T/T_c}, \quad (t \rightarrow \text{sufficiently large}). \quad (17)$$

As long as $t \ll w_{\max}$, $\Xi(t)$ remains almost constant as t increases. Once t becomes comparable with w_{\max} , however, $\Xi(t)$ decreases appreciably with the increase in t (the relation between t and $\Xi(t)$ is given for $T/T_c = 1$ in Table 2 as an explanation example. For this reason, C_{out} eventually deviates from the power law. We emphasize, however, that w_{\max} should be extremely large in many cases and the feature of the response curve is definitely anomalous in the sense that it cannot be elucidated by a conventional theory. In fact, the response curves measured for Ba^{2+} exhibit no departure from the power law until C_{out} decreases to the detection limit of the analytical device used (the power law does hold until $t \gtrsim 5 \times 10^4$ min).

Conclusions

We have performed a new set of response experiments for the system of cations (Sr^{2+} and Ba^{2+}) plus activated charcoal. It has been verified that adsorption sites predominate over dead-end pores or spaces as trappers. For each of the cation species (Sr^{2+} and Ba^{2+}), the exponent α varies nearly in proportion to the absolute temperature as suggested by Eq. 2. α is independent of the water flow rate, bed length, and initial concentration of solute molecules or ions. Thus, the agreement between theoretical prediction and experimental observation in terms of the dependency of α on the experimental conditions is very good.

The power law observed is ascribed to the fractal-like feature of the desorption process. According to our theory, the feature stems from the following two factors: (i) the residence-time of a solute molecule (or an ion) adsorbed on a site having a certain activation energy cannot uniquely be determined because the desorption is a stochastic process; (ii) the activation energy varies from site to site, obeying a completely random distribution.

C_{out} measured for Sr^{2+} eventually deviates from the power law, decreasing more rapidly than the law predicts. This deviation can be explained by introducing the assumption that there exists a maximum value of the activation energy E_{\max}

for the desorption. On the other hand, C_{out} measured for Ba^{2+} does not show such deviation, and E_{\max} in this case should be virtually infinite. We emphasize, however, that the power law does hold for a very long time in either case, and the behavior of the mass-transport process cannot be elucidated by a conventional theory.

One might think that the power law observed stems from the situation that adsorption equilibrium always holds between aqueous solution and activated charcoal and the equilibrium relationship is expressed by the Freundlich equation. However, this thought should be set aside because it gives a dependency of α on the operating temperature which is opposite to the experimental observation.

There is no guarantee that all of the previously reported theories in the vast engineering literature on chromatographic columns and packed adsorbents fail to describe the results of our response experiments. However, our theoretical approach is unique in the respect that it accounts for the nonhomogeneity of the sorbing media and reveals the fractal-like feature of the desorption process. Comparing our approach in detail with conventional ones is a task for the future.

We expect that our model (or theoretical approach) can be applied to subjects such as the transport phenomena inside the porous polymeric membranes and porous glasses, the migration of radioactive nuclides through the geologic sorbing media, and the regeneration of the adsorbents.

Acknowledgment

The present study was performed as part of the "Studies on Safety Evaluation for Solidified Nonvolatile Nuclides and Design of Nuclide Separation System," supported by a Grant for Special Projects from the Ministry of Education, Science, Sports and Culture of Japan.

Notation

- C_i = concentration of i ($i = \text{Sr}^{2+}$ or Ba^{2+}) in aqueous solution, ppm
- C_{in} = initial concentration of cations, ppm
- E = activation energy for desorption defined for a site, J/mol
- $h(w)$ = distribution function for desorption rate constant defined for adsorption sites, 1/min
- K_i = constant in the Freundlich equilibrium relation, $X_i = K_i C_i^m$, $\text{mg}/(\text{g} \cdot \text{ppm}^m)$
- k = constant in the Freundlich equilibrium relation, $n_s = k n_w^m$, $\text{mol}^{(1-m)}/\text{cm}^{3(1-m)}$
- L = length of the media, cm
- n_w = ionic concentration in aqueous solution at the outlet of the vessel, mol/cm^3
- $n_{w,0}$ = initial value of n_w , mol/cm^3
- n_w^{in} = ionic concentration in aqueous solution at the inlet of the vessel, mol/cm^3
- n_s = ionic concentration in activated charcoal, mol/cm^3
- $P(x, t)$ = density of solute molecules moving with the fluid flow at point x in the media at time t , mol/cm^3
- $P_1(x, t)$ = density of solute molecules being trapped on adsorption sites at point x in the media at time t , mol/cm^3
- $q(E)$ = distribution function for activation energy defined for adsorption sites, mol/J
- Q = flow rate of aqueous solution, cm^3/s
- R = gas constant, $\text{J}/(\text{mol} \cdot \text{K})$
- S = cross-sectional area of the packed bed, cm^2
- V_0 = volume of a vessel, cm^3
- X_i = amount of ionic species i ($i = \text{Sr}^{2+}$ or Ba^{2+}) adsorbed on activated charcoal, mg/g
- ϵ = void fraction of the packed bed
- ϵ_v = void fraction of the vessel

ϕ_1 = residence-time distribution function for a solute molecule adsorbed on a site, 1/min
 ω = transfer rate constant for solute molecules from the fluid to adsorption sites, 1/min

Literature Cited

- Domb, C., "The Percolation Phase Transition," *Annals of the Israel Phys. Soc.: 5. Percolation Structures and Processes*, G. Deutscher, R. Zallen, and J. Adler, eds., Israel Physical Society, Jerusalem, Israel, p. 17 (1983).
- Freeman, G. R., *Kinetics of Nonhomogeneous Processes*, Wiley, New York (1987).
- Kinoshita, M., M. Harada, M. Kishida, and Y. Nakamura, "Fractal-Like Behavior Observed for a Mass-Transport Process," *AIChE J.*, **38**, 1667 (1992).
- Kopelman, R., "Rate Processes on Fractals: Theory, Simulations, and Experiments," *J. Stat. Phys.*, **42**, 185 (1986).
- Kopelman, R., et al., *Dynamical Processes in Condensed Molecular Systems*, J. Klafter et al., eds., World Scientific, Singapore, p. 231 (1989).
- Noolandi, J., "Multiple-Trapping Model of Anomalous Transit-Time Dispersion in a-Se," *Phys. Rev. B*, **16**, 4466 (1977).
- Noolandi, J., "Equivalence of Multiple-Trapping Model and Time-Dependent Random Walk," *Phys. Rev. B*, **16**, 4474 (1977).
- Plonka, A., "Time-Dependent Reactivity of Species in Condensed Media," *Lecture Notes in Chemistry*, Vol. 40, Springer-Verlag, Berlin (1986).
- Pfister, G., and H. Scher, "Dispersive (non-Gaussian) Transient Transport in Disordered Solids," *Adv. Phys.*, **27**, 747 (1978).
- Scher, H., and E. W. Montroll, "Anomalous Transit-Time Dispersion in Amorphous Solids," *Phys. Rev. B*, **12**, 2455 (1975).

Appendix: Derivation of Eq. 15

Here, we assume that adsorption equilibrium always holds between aqueous solution and activated charcoal and the equilibrium relationship is expressed by the Freundlich equation. It is mathematically easier to consider the continuous stirred vessels model.

For the first vessel, the material balance equation is expressed by

$$d\{\epsilon_v n_w + (1 - \epsilon_v) n_s\} / dt = -(Q/V_v) n_w \quad (A1)$$

Substituting the Freundlich equation (this is equivalent to $X_i = K_i C_i^m$)

$$n_s = k n_w^m \quad (0 < m < 1) \quad (A2)$$

into Eq. A1 yields

$$dn_w/dt = -(Q/V) n_w \{ \epsilon_v n_w + (1 - \epsilon_v) k m n_w^{(1-m)} \} \quad (A3)$$

Solving Eq. A3 with the initial condition, $n_w = n_{w0}$ at $t = 0$, yields

$$\epsilon_v \ln(n_w/n_{w0}) - \{(1 - \epsilon_v) k m / (1 - m)\} \times \{n_w^{-(1-m)} - n_{w0}^{-(1-m)}\} = -(Q/V) t \quad (A4)$$

It can readily be shown that

$$t \rightarrow \infty: n_w \rightarrow t^{-1/(1-m)} \quad (A5)$$

For the second vessel, the material balance equation is expressed by

$$d\{\epsilon_v n_w + (1 - \epsilon_v) n_s\} / dt = (Q/V)(n_w^{\text{in}} - n_w) \quad (A6)$$

From Eq. A5

$$t \rightarrow \infty: n_w^{\text{in}} \rightarrow t^{-1/(1-m)} \quad (A7)$$

Hence, as $t \rightarrow \infty$

$$dn_w/dt = \{a_2 t^{-1/(1-m)} - a_3 n_w\} / \{1 + a_1 n_w^{-(1-m)}\} \quad (A8)$$

where a_1 , a_2 and a_3 are constants. Here, we assume that $n_w \rightarrow a_4 t^{-j}$ as $t \rightarrow \infty$ (a_4 is a constant j is a positive exponent). It then follows that

$$\begin{aligned} -a_4 j t^{-j-1} &= \{a_2 t^{-1/(1-m)} - a_3 a_4 t^{-j}\} / \{1 + a_5 t^{j(1-m)}\} \\ &\rightarrow a_6 t^{-1/(1-m)-j(1-m)} - a_7 t^{-j-j(1-m)} \end{aligned} \quad (A9)$$

where a_5 , a_6 and a_7 are constants. Hence, $j = 1/(1-m)$ and

$$t \rightarrow \infty: n_w \rightarrow t^{-1/(1-m)} \quad (A10)$$

The same analysis can be performed for the n th vessel ($n = 3, 4, \dots$), and it is now clear that irrespective of the total number of vessels Eq. A10 does hold and

$$C_{\text{out}} \sim t^{-\alpha}, \quad (t \rightarrow \text{sufficiently large}), \quad \alpha = 1/(1-m) \quad (A11)$$

Manuscript received May 28, 1996, and revision received Jan. 13, 1997.